Chapter 6
Sensing Single Protein Molecules with Solid-State Nanopores

Bradley Ledden, Daniel Fologea, David S. Talaga, and Jiali Li

Abstract This chapter is focused on the development of experiments and theory of using solid-state nanopores for sensing single protein molecules in their native and unfolded states. Proteins serve diverse roles such as transport carriers, catalysts, molecular motors, cellular structural support, and others that make life possible. Because of these widely differing roles, proteins have an enormously diverse set of shapes, sizes, and charge structures as compared to polynucleic acids. Solid-state nanopores are particularly suitable for characterizing single protein molecules because they can be fabricated with adjustable dimensions and are stable under conditions that denature proteins. This chapter describes the nanopore experimental setup, signal recording, data analysis, and basic principles related to the experiments and the theory connecting the electrical signal with the properties of proteins. Examples of experimental results illustrate the ability of solid-state nanopores to differentiate proteins in their folded and unfolded states. Native-state protein nanopore translocation follows biased one-dimensional diffusion of charged particles that is sensitive to size and electrical charge. Due to the heterogeneous charge sequence of polypeptides, unfolded proteins obey a coupled electrophoretic and thermally activated process that is sequence specific. The chapter concludes with a discussion of future directions and open challenges for single protein characterization using solid-state nanopores.

Keywords Protein capture • Protein shape during translocation • Protein's Charge variation with pH • Parameters affecting translocation

J. Li (✉)
Department of Physics, University of Arkansas, 226 Physics Bldg.,
Fayetteville, AR 72701, USA
e-mail: jialili@uark.edu

S.M. Iqbal and R. Bashir (eds.), *Nanopores: Sensing and Fundamental Biological Interactions*, DOI 10.1007/978-1-4419-8252-0_6,

6.1 Introduction

The combination of variable polypeptide sequence and nearly arbitrary chain length results in an astronomical number of possible proteins. The resulting variety of structures and functions of proteins are so complicated that in some ways the diversity of life on Earth can be viewed as a consequence thereof. Eukaryotic life forms must transport functional biopolymers across membranes to survive. This fact motivates study of protein translocation through nanometer-scale pores. Such understanding is of fundamental importance not only for basic science but also in biotechnological applications that seek to mimic the selectivity and sensitivity of biological translocation [1, 2].

The physiochemical properties of the two most important classes of biopolymers, polynucleic acids and polypeptides, are substantially different. Therefore the cellular transport machinery is different depending on the nature of the biopolymer being transported. Proteins in particular present special challenges for cells, as they must be transported in a way that is compatible with attainment of a correctly folded three-dimensional native structure. The experimental and theoretical approaches to both natural and artificial ion channel translocation must accommodate these differences.

In this chapter we summarize the recent development of single nanopore measurements and theory to enable measurement of the physical properties of proteins at the single molecule level. These physical properties include: the protein size or volume, electrical charge, and conformational states.

6.1.1 Polypeptides Measured by Protein Pores

Protein channels or protein pores such as α-hemolysin have well defined structure and dimensions. However, due to their small fixed diameter, only polypeptides or denatured proteins are able to pass through the pores. Several research groups have studied polypeptide and protein pore interactions and the results have been presented in many publications. Starting in the 1990s, experiments began revealing that some peptide chains could reside inside in the lumen of protein pores or channels [3]. Later, studies in Lee's lab demonstrated that resistive pulse signals from a single α-hemolysin pore could differentiate between single, double, and collagen-like triple helices and pulses from α-hemolysin or aerolysin pores could reveal differences between wild type and mutant Histidine containing protein [4, 5]. The Auvray and Pelta research groups have studied the interaction of dextran sulfate and maltose binding protein with α-hemolysin pores [6, 7]. The Movileanu and Bayley laboratories have used wild type and mutated α-hemolysin pores to examine the effect of electrostatics on the interaction between peptide sequences and the α-hemolysin pore [8, 9].

6.1.2 Proteins Measured by Solid-State Nanopores

Solid-state nanopores are capable of measuring proteins of any conformation or size due to their tunable dimensions. Using 30–55 nm diameter, 20 nm thick nanopores formed by *e*-beam lithography in a free standing silicon nitride membrane, Han et al. measured bovine serum albumin (BSA), ovalbumin, avidin, streptavidin, human chorionic gonadotropin β (β-HCG), and monoclonal anti-β-HCG proteins [10, 11]. Using ~15 nm diameter silicon nitride nanopores, Fologea et al. compared the current blockage signal of BSA with fibrinogen, and measured the pH dependence of the BSA current blockage signal. In this work we confirmed that BSA indeed translocated through a nanopore using a chemiluminescent method [12]. Talaga and Li have studied unfolding of bovine β-lactoglobulin variant a (βLGa) and Histidine-containing phosphocarrier protein (HPr) [13]. Recently, Firnkes et al. reported on translocation of avidin [14], and Niedzwiecki et al. have reported on the adsorption of BSA in silicon nitride nanopores [15].

6.1.3 Parameters to Be Measured in a Nanopore Experiment

As illustrated in Fig. 6.1a, the main component of a nanopore sensing system is a single nanopore in a silicon nitride membrane separating two chambers connected electrically only by the electrolyte solution inside the nanopore. When a voltage is applied across the membrane, negatively (or positively) charged protein molecules added to the *cis* chamber near the nanopore are captured by the electric field, and driven through the nanopore to the positively (or negatively) biased *trans* chamber.

The translocation process of a protein molecule in a nanopore can be quantitatively described in terms of the nanopore and protein geometries. The geometric parameters required are illustrated in Fig. 6.1a and are: the average diameter (d_m) and the length (l_m) of a protein molecule, the mean diameter (D_p) or area (A_p) and the effective thickness (H_{eff}) of a nanopore.

At the macroscopic level, a nanopore's electrical behavior in an electrolyte solution of conductivity σ obeys Ohm's Law for an electrolytic resistor to good approximation. For an approximately cylindrical nanopore under applied voltage Ψ, the open pore current measured when the nanopore is not occupied by a protein molecule is $I_o = \Psi/R_0 = \Psi\sigma A_p/H_{eff}$. When a protein molecule is in the nanopore, it partially blocks the flow of ions [Fig. 6.1a, b (right)] producing a transient decrease in the open pore current. The current trace in Fig. 6.1c was recorded when a laminin (L6274, Sigma-Aldrich) protein sample was added to the *cis* chamber. The pH 7 electrolyte solution contained 1 M KCl and 3 M guanidine. The laminin protein was partially denatured in 3 M guanidine. The *trans* chamber was negatively biased for the recording; laminin is positively charged at pH 7.

Each current blockage event in Fig. 6.1c represents a laminin protein molecule interacting with or translocating through the nanopore. The transient decrease in

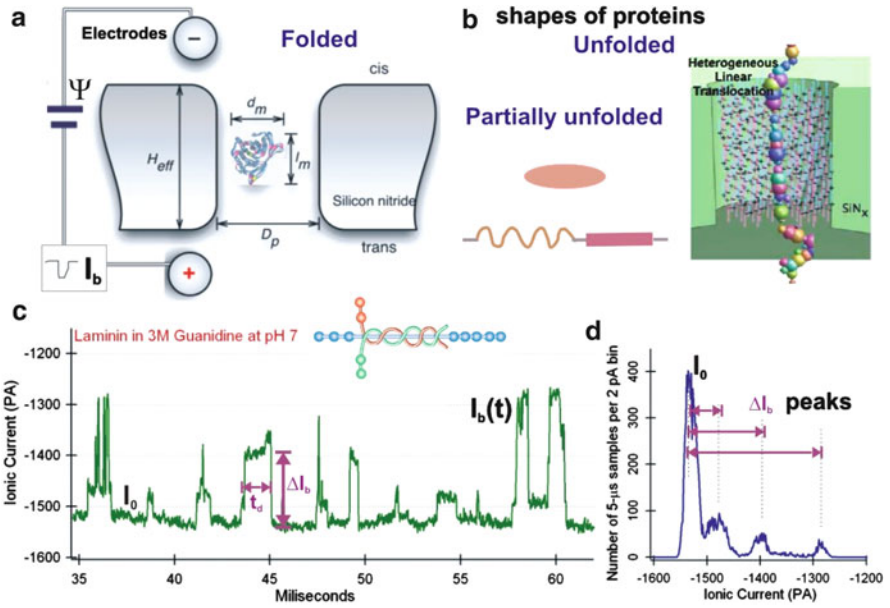

Fig. 6.1 (**a**) Schematic diagram of protein nanopore translocation experiment. (**b**) Illustration the shapes of proteins and an unfolded protein translocation in a nanopore. (**c**) Several recorded Laminin (L6274, Sigma-Aldrich) current blockage events in partially denatured condition (in 3 M Guanidine HCl at pH 7 and 1 M KCl). The insert is an illustrated structure of Laminin at its native state (taken from http://www.sigmaaldrich.com). (**d**) The Ipoint histogram or the instantaneous time distribution of blockade current ΔI_b over all events

ionic current caused by the translocating protein is a time dependent quantity, $\Delta I_b(t)$. Separating the translocation-relative variability in $\Delta I_b(t)$ from the noise-related variability in $\Delta I_b(t)$ is an ongoing challenge. In this chapter, we consider the mean current blockage amplitude ΔI_b and the dwell time t_d while a protein molecule stays in a nanopore.

6.1.4 Event Classification

Analysis of protein translocation current blockage events has been a challenging task due to their complexity. For initial analysis of a data set, we usually first generate the instantaneous time distribution of blockade current ΔI_b over all events (Fig. 6.1d), called I_{point} histogram [16]. The I_{point} histogram can help us to identify possible peak values of ΔI_b that can be used to set a trigger line to classify events. To classify events, a MATLAB based program has been developed. Using a trigger line at approximately half the value of an interested peak, the MATLAB program can select a group of events, calculate the mean blockage current ΔI_b and the time duration t_d of each event. When the current, $I(t)$, crosses the trigger line the event is considered to start, and the event stops when the current crosses the trigger line again. The time difference between the stop and start times is calculated as the

event duration t_d. The average current of all points between the start and stop times is calculated as ΔI_b. The events with t_d that are very short (beyond the time resolution of the measuring system) and too long are discarded.

6.2 Principles of Protein Translocation

The translocation of proteins through nanopores differs from that of the more commonly studied polynucleic acids. The physical properties of proteins differ from those of polynucleic acids in several important ways that directly impact their nanopore capture, insertion, and translocation. These differences result in changes in data analysis and interpretation for protein translocation in nanopores.

6.2.1 Protein Capture by Nanopores

A charged molecule near the entrance of a properly biased nanopore will be captured. Entrance into the pore depends on the molecule's ability to attain a sterically compatible geometry for translocation during its encounter with the nanopore opening. For a polynucleotide this typically requires threading one end of the chain or forming a bend in the chain. Since a polynucleotide is uniformly charged, bend insertion can occur essentially anywhere in the sequence. By contrast, proteins have both pre-formed loops and charges of both sign distributed along their length suggesting that particular locations of bend insertion will be preferred. Protein C and N termini can have opposite polarity and therefore may also exhibit selectivity during the insertion event.

6.2.2 Protein Shape or Geometry During Translocation

In contrast to polynucleotides, proteins most often have a single well-defined three-dimensional native-state structure. This structure can be partly or completely disrupted by denaturants, temperature, or the application of electric fields. Tertiary contacts in proteins can be stabilized by both covalent and non-covalent interactions. Thus, the structure of the protein during translocation can be globular (Fig. 6.1a), looped, or a completely unfolded linear chain and (Fig. 6.1b) depending on the conditions during the measurement.

When the protein translocates as a loop or linear chain, only a segment of the amino acid chain will typically be inside the nanopore (Fig. 6.1b) and be exposed to the influence of the electric field therein. The molecular volume of amino acids varies much more than that of nucleotides. As a result, the magnitude of the current drop can vary more for proteins and is potentially more sensitive to particular features in the sequence. Moreover the distribution of charges along the polypeptide chain is sequence dependent; the net charge inside the pore can fluctuate as a function of translocation position. The net electrical driving force can change

direction when the net charge of the local segment changes sign, which could drive the protein back and forth near the electrically neutral charged region. The polypeptide chain could be transiently stalled or trapped in an electrical potential well due to protein heterogeneous charge sequence.

The variability of protein physical properties influences the behavior of the main translocation observables derived from nanopore resistive pulse measurements. The complexity in the translocation physics of proteins is reflected in both the mean current drop and current blockage duration (translocation time).

6.2.3 The Mean Current Drop Amplitude of an Event

The intrusion of a protein or a polypeptide segment into the nanopore reduces its current flow capacity. To relate the transient current blockage amplitude ΔI_b to the physical properties of protein molecules, Ohm's law can be exploited based on the volume displacement of the electrolyte solution from the pore [17–20]. A translocating molecule that is much smaller than an idealized cylindrical nanopore will cause a transient drop in current that can be written as

$$\Delta I_b(t) = -I_0 \frac{\Lambda(t)}{H_{eff} A_p} [1 + f(d_m/D_p, l_m/H_{eff})] \tag{6.1}$$

when the nanopore accounts for nearly all the resistance in the circuit. Here $A_pH_{eff}=V_p$, the volume of the pore and $f(d_m/D_p, l_m/H_{eff})$ is a correction factor that depends on the shape of a protein molecule and the relative values associated with the dimensions of a molecule and a nanopore. (Note, this equation neglects nanopore surface charge effects, which might be significant at low salt concentrations [21].) The correction, f, contains higher order terms in the ratios of the molecule to pore diameter (d_m/D_p) and molecule to effective pore length (l_m/H_{eff}) [18]. For example, $f(d_m/D_p, l_m/H_{eff})=(4/5)(d_m/D_p)^2$ for a spherical shaped particle that is smaller than the pore but not at the small particle limit [18]. For short molecules that fit entirely inside the length of the pore like small folded proteins, these ratios are less than one and contribute little to the current drop [18, 22–24]. For molecules such as polynucleotides and unfolded proteins that are much longer than the pore, a different derivation based on Ohm's law produces a relation that contains only the first term for the absolute, $\Delta I_b \approx I_0(\Lambda/V_p)$, or relative current drop, $\Delta I_b/I_0 \approx \Lambda/V_p$. These equations relate the measured current drop amplitude to the volume of the molecule transiently blocking the pore.

Equation (6.1) shows that the instantaneous excluded volume of a molecule, $\Lambda(t)$, can be estimated by measuring $\Delta I_b(t)$, however the correction term will vary depending on the conformation of the protein during the translocation which can vary as shown in Fig. 6.1b. A folded globular protein will require a correction appropriate for a spherical or ellipsoidal particle (Fig. 6.1a) and the expected current drop is larger than for a linear particle with the same volume inside the nanopore. The partially unfolded, and completely unfolded protein translocations will be

closer to the linear case where the correction, $f(d_m/D_{p,}\ l_m/H_{eff}) \sim 0$. However, even in the linear case, the variability of the amino acid side chain volume suggests that there will be instantaneous excluded volume $\Lambda(t)$ changes as illustrated in Fig. 6.1b.

6.2.4 Protein Translocation Times

The time it takes for a charged protein molecule to pass a voltage biased nanopore or the dwell time, t_d, involves many phenomena. To simplify the problem, here we first assume protein molecules are rigid particles with a total charge Q and once the molecules enter the pore, they move along the center line of the pore of length H_{eff} under the electrical field strength $E = \Psi/H_{eff}$, and we further ignore complex issues such as protein-pore interactions and electro-osmotic flow. Under these assumptions, the total force exerted on a protein molecule is the electric driving force opposed by a viscous drag plus a term of random force caused by collision with molecules in solution, we can approximate the translocation time with a 1-D Langevin equation,

$$m\frac{dv}{dt} = F_e(x) - F_{drag} + kW(t) \tag{6.2}$$

where v is the velocity of the molecule, $F_e = Q_{in}\Psi/H_{eff}$ is the driving force due to the electric field, $F_{drag} = \alpha v$ where α is the drag coefficient related to the diffusion coefficient by $\alpha = k_bT/D$, k is defined by the fluctuation-dissipation theorem, and $W(t)$ is a 'noise term' or Wiener process that represents the random thermal forces on the molecule. The variable x is the position of the first part of the molecule that enters the pore.

If we assume a protein molecule translocate a nanopore with a terminal or an average speed, $dv/dt = 0$, and the average dwell time (mean first passage time) t_d is long, the mean value of the fluctuating force is zero, then $F_e(x) = F_{drag}$. Using this approximation, we can derive the translocation time for a uniformly charged long chain polymer like a DNA molecule and a charged globular shaped protein molecule.

Globular protein translocation. If the passing protein molecule is much smaller ($d_m << D_p$, $l_m << H_{eff}$) than the pore, and if we assume the interaction between a protein molecule and the pore can be neglected (i.e. free translocation), and further we assume the protein translocation process is driven by an electrophoretic force, $F_e = Q\Psi/H_{eff}$, opposed by a viscous drag, $F_{drag} = \alpha v = \eta C_f v$, with a terminal speed $v = H_{eff}/t_d$, the t_d can be written as

$$t_d = C_f \frac{\eta H_{eff}^2}{Q\Psi} \tag{6.3}$$

Here $\alpha = \eta C_f$ is the friction coefficient, η is the solution viscosity, C_f is a constant for a protein in a specific shape, and Q is the total net effective charge of a protein.

Both ΔI_b and t_d (Fig. 6.1c) also depend on the geometry and electrical properties of a nanopore, on the properties of solution, and the bias potential.

The distribution function for the translocation time can be derived from the Fokker-Planck equation equivalent to Eq. (6.2) [13].

$$P_{fpt}(t) = \frac{e^{-\frac{(d-tv)^2}{4tD}}(d+tv)}{t\sqrt{4\pi tD}} \tag{6.4}$$

Here d is the distance to be translocated. For a long polymer with $l_m >> H_{eff}$, $d = l_m + H_{eff}$; for a small spherical particle $d = H_{eff}$. In this formulation, the width of the distribution arises due to thermal fluctuations. Equations (6.3) and (6.4) are appropriate for uniformly charged polymers and particles that behave as a point charge. The prediction under these assumptions is that the translocation time should decrease when electrostatic bias across the nanopore is increased.

When a protein molecule is unfolded and it passes a nanopore as a linear amino acid chain, very different translocation kinetics is expected due to the inhomogeneous charge distribution. A protein molecule that has neutral regions bracketed by a positively charged and a negatively charged region can experience a net zero electrical force when the net charge of the local segment chain in the pore is zero. At this stall point the unfolded protein molecule is electrostatically trapped; increasing the voltage only serves to increase the electrostatic trap barrier height. The molecule can escape the trap by thermal fluctuations, thus an inhomogeneous charge polymer translocation could be thermally activated if it has zero net charged regions. Since larger applied bias voltages, Ψ, would result in deeper traps, the dwell time, t_d, is predicted to increase with Ψ, the opposite prediction from the uniformly charged translocation model of Eqs. (6.3) and (6.4). The consequences of unfolded protein translocation are discussed below, in context with the experimental evidence.

6.3 Experimental Setup and Sample Preparation

6.3.1 Experimental Setup

The results discussed in this chapter were measured with a solid-state nanopore sensing system as illustrated in Fig. 6.2a. The main components of this system include a nanopore chip, two PDMS chambers (*cis* and *trans*), a pair of Ag/AgCl electrodes, and an Axopatch (200B) single channel recording system. The nanopore chip has a dimension of 3 mm by 3 mm and is sandwiched between two PDMS chambers. A freestanding silicon nitride membrane widow supported by a silicon substrate contains a single nanometer size pore at the center of the chip. The thickness of the freestanding membrane is ~275 nm as illustrated in the expanded view of the region around the pore in Fig. 6.2b. The nanopore is the

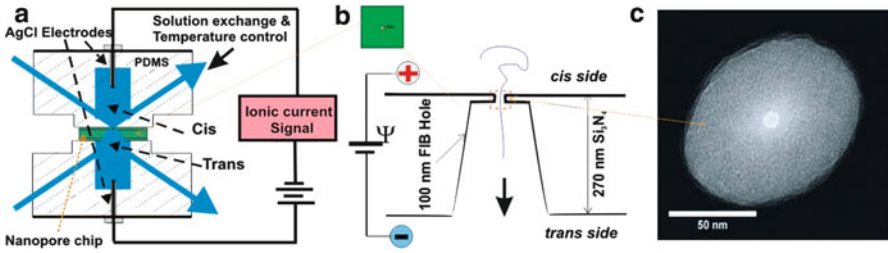

Fig. 6.2 (**a**) The Schematic of a solid-state nanopore detection system for protein translocation experiments. (**b**) The nanopore cross-section profile (across the center) illustrated. (**c**) An ion beam sculpted ~8 nm diameter pore imaged by TEM

only connection between two electrolyte filled chambers. The bandwidth of the Axopatch 200B was set at 10 or 100 kHz depending on the time duration of the protein signal and noise level of the nanopore.

6.3.2 Solid-State Nanopore Fabrication

Solid-state nanopores have been fabricated by low energy ion beams and by electron beams [25, 26] with several insulating materials such as silicon nitride [27, 28], silicon dioxide [29, 30], and aluminum oxides [31, 32]. The data discussed in this chapter were measured with silicon-nitride nanopores made by low energy noble gas ion beams. The typical size of nanopores used for protein measurements are between 4 and 30 nm selected according to the size and conformational states of proteins to be measured. Practically, nanopores with diameters 2–3 times larger than the protein are better choices for sensing protein molecules. The 275 nm low stress silicon nitride membrane was deposited by LPCVD at CNF (Cornel Nanofabrication Facility). The freestanding membrane window was created by photolithography, reactive ion etching, and anisotropic wet KOH etching. A single ~100 nm hole or a FIB hole (Fig. 6.2b) is milled through the freestanding membrane by a 50 keV Ga ion beam from a focused ion beam machine. The nanopores are made by shrinking the ~100 nm FIB hole to a desired diameter using low energy noble gas ion beam sculpting [27, 29, 33, 34]. The nanopores made by this method have a length or thickness between 10 and 20 nm depending on ion beam parameters selected [34]. A TEM image of a nanopore made by this method is shown in Fig. 6.2c.

6.4 Measuring Native State Proteins

The volume (Λ) a protein molecule occupies in space or solution is approximately proportional to the protein's molecular weight (M) or size, $\Lambda \propto M$. When a protein molecule is at its native or folded state and if the protein length is smaller than the

nanopore, $l_m < H_{eff}$, the measured current blockage amplitude ΔI_b is expected to be directly proportional to the excluded volume Λ of a protein molecule as described in Eq. (6.1). In addition, when a native state protein molecule is passing through a nanopore driven by an electric field, the time duration t_d is expected inversely proportional to its electrical charge Q as described in Eq. (6.3). In this section, based on our experimental results and data analysis, we discuss the resolution of using ion beam sculpted silicon nitride nanopores on measuring a protein's size and relative electrical charge.

6.4.1 Sizing Protein Molecules

Figure 6.3 demonstrates the use of a solid-state nanopore to measure and discriminate the size of native state proteins. Using a 22 nm nominal diameter pore, three different proteins were measured sequentially: BSA (66.4 kDa, 607 aa, −18 *e*), Fibrinogen (340 kDa, ~1,500 aa, −16 *e*), and Laminin M (850 kDa, ~3,110 aa, +34 *e*). Event density plots in Fig. 6.3a, b, c show that the current blockage amplitude was correlated to protein size (Fig. 6.3d): ΔI_b (Laminin)=84 pA > ΔI_b (Fibrinogen)= 74 pA > ΔI_b (BSA)=50 pA. Figure 6.3e shows that the time duration followed the same trend: t_d(Lam)=154 μs > t_d(Fib)=101 μs > t_d(BSA)=64 μs. Laminin has twice the electrical charge than BSA and Fib but its t_d is the longest, which suggests that the time t_d depends on both the electrical charge and molecular size, t_d ~Λ/Q,

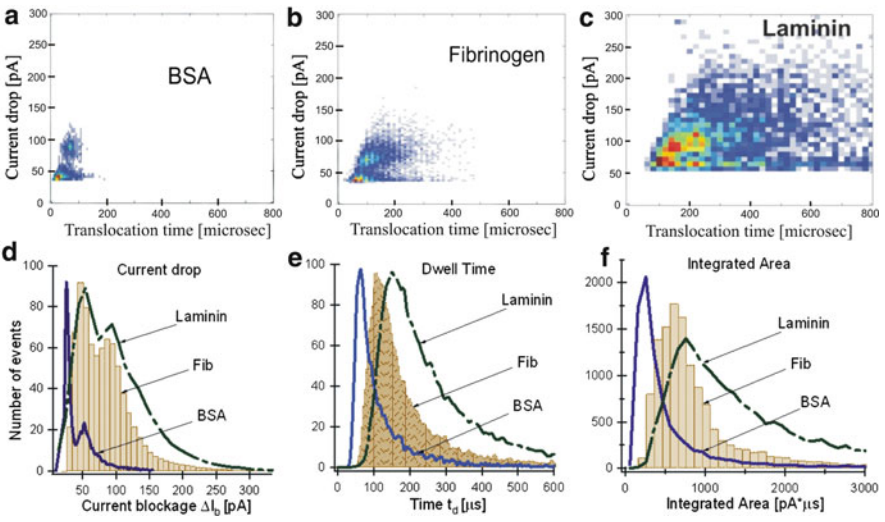

Fig. 6.3 Event Number density plots for BSA (**a**), Fibrinogen (**b**), and Laminin (**c**) in 1 M KCl, 40% Glycerol, pH=7. The current drop (**d**), time duration (**e**), and the integrated area of events for all three proteins (**f**). The pore used was 22 ± 2 nm made by Ar at 3 kV. The low pass filter was set at 100 kHz for this set of data

possibly due to an increased drag force when the molecular volume is larger. The integrated area histogram (Fig. 6.3f) is a measure of total charge of ions in solution displaced by the protein, $A_{ecd} = \int_{event} \Delta I_b(t)dt$, and clearly shows that the nanopore measurement differentiated these three proteins. Even though BSA and Fibrinogen had similar total charges (−16 e vs −18 e at pH=7.0), the difference in their molecular weights (and therefore volumes) allowed the current drop signals of fibrinogen to be clearly differentiated from those of BSA [12].

Advantages of using solid-state nanopores to characterize native state proteins include that the measurement is performed in aqueous salt solution and no marker or modifications of proteins are required. However, the data also show resolution in sizing different native state proteins is relatively low. One possible reason for this is that the distribution of the peaks including both ΔI_b and t_d are broad, limiting the precision of the excluded volume measurement. Another possible limitation in application to native state proteins is that most proteins have positive and negative charged residues. In the strong electric field in a nanopore, positive and negative charges will be driven to opposite directions possibly inducing structural changes in native state proteins. Both transient and long-lived structural changes could occur and the contribution of these phenomena to the nanopore events has yet to be fully characterized. When present, these nanopore-induced conformational changes could lead to systematic bias in the estimation of the volume Λ when using Eq. (6.1).

6.4.2 Measuring a Protein's Relative Charge at Different pH

Native state proteins, depending on their structure and charge distribution, can be partially or fully unfolded by the strong electrical field strength (~10^5V/cm) in a nanopore [35]. However, proteins with many disulfide bonds are the most likely to maintain their native state form during electrophoretic translocation. Native state BSA has 17 disulfide bonds, which should make it relatively stable in a nanopore; it is expected to behave like a simple charged particle during translocation and not experience large long-lived conformational changes [36]. Therefore BSA is a good model system for measuring the electrical charge change as a function of pH.

BSA (Fig. 6.4a) has an isoelectric point (pI) ranging from pH 5.1–5.5 [37]. The protein has an overall negative charge (−18 e) at pH 7. The charge of BSA can be altered by varying the pH of the solution. Using a ~16 nm diameter pore in a solution of 0.5 M KCl at pH 7.0, with ψ=120 mV, I_0 ~ 7.4 nA was measured. After addition of BSA to the negatively biased *cis* chamber, downward blockage events occurred (Fig. 6.7a) indicating that BSA molecules were negatively charged. When the *cis* chamber was positively biased, no blockage events were observed at the beginning of the experiment. The cumulative results are presented in an event number distribution plot (Fig. 6.7d).

When the solution pH of the chambers was lowered to acidic conditions (pH $<$ 5) below the pI of BSA, current blockages disappeared if the *trans* chamber remained

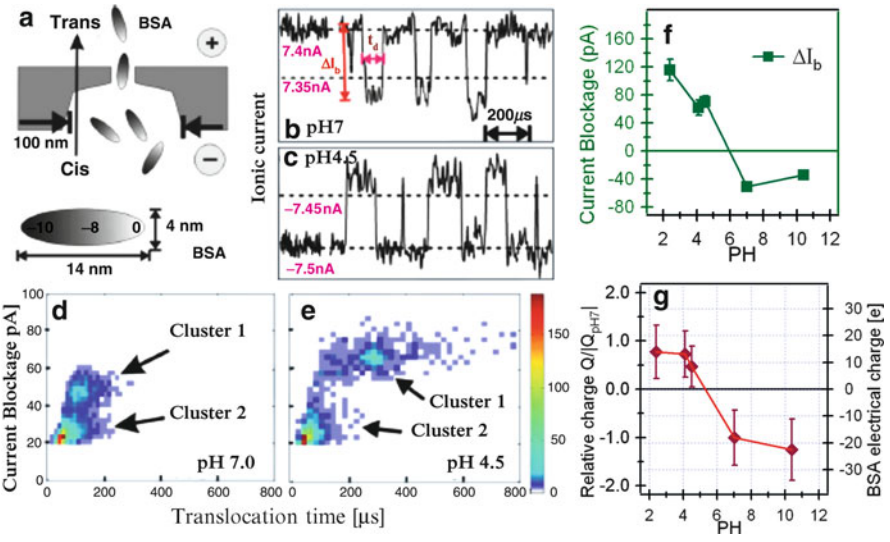

Fig. 6.4 BSA protein in 0.5 M KCl solution measured as a function of pH at ψ=120 mV. Panel (**a**) shows a sketch of BSA translocation through a solid-state nanopore with BSA dimensions shown. Panel (**b**) shows current drops due to BSA translocation at pH 7. Panel (**c**) shows the current drops from BSA translocation at pH 4.5. Note that BSA is positively charged and the bias across the nanopore has been reversed. Panels (**d**) and (**e**) are density plots of BSA translocation through a solid-state nanopore at these two different pH values. (**f**) The most probable values of ΔI_b, (**g**) the relative BSA electrical charge to pH 7. The open pore current was I_0~7.4 nA at ψ=120 mV for all pHs measured

positively biased. However, when the *trans* chamber was switched to negative bias, current blockages appeared again as shown in Fig. 6.7c, indicating the net charge of BSA protein had changed to positive at pH $<$ 5. This measurement is consistent with the fact that BSA is positively charged when the pH is lower than its pI [38]. We studied the translocation of BSA through the same nanopore at three different acidic pH values (4.5, 4.1 and 2.4). The BSA molecules proved to be positively charged at all these pH values. When the pH was 4.5, near the pI of BSA, the most probable values are ΔI_b~71 pA and t_d ~269 μs as shown in Fig. 6.7e. The same measurement was performed at a higher pH value of 10.4. The most probable values of ΔI_b (Cluster 2 events were used) varied as solution pH changed (Fig. 6.4f) indicating the shape of the BSA molecule was not the same. The open pore current I_0 was approximately a constant at all the pH values measured.

A decrease in ΔI_b (Fig. 6.4f) suggests that the local excluded volume Λ of BSA molecules decreased at higher pH indicating a change in conformation or dimensions of BSA molecules took place. These results are consistent with reports of BSA denaturation at high pH, and formation of dimers at low pH [39] or BSA volume expansion at acidic pH [37]. A change in the charge of BSA (Q) can be estimated by the change in t_d. The relative charges Q/Q_{pH7} estimated from Eq. (6.3) are shown in Fig. 6.4g. A pI $\approx$ 5.3 was estimated for the BSA by this nanopore experiment.

This result demonstrated that a nanopore measurement is sensitive to the electrical charge of proteins and can be used to probe the pI of an unknown native state protein in an aqueous solution close to their native conditions.

6.5 Linear Amino Acid Chain Translocation

The electrophoretic force on an unfolded protein will tend to stretch it out during translocation. If the chain length l_m is longer than the pore length H_{eff}, only a segment of the chain is occupying the pore as illustrated in Figs. 6.1b and 6.5a. The electrophoretic translocation kinetics of a driven linear amino acid chain is expected to depend on the details of the primary sequence of charged amino acids rather than the total net charge as is the case for a globular proteins (Fig. 6.1a) or polynucleic acids. Using bovine β-lactoglobulin variant a (βLGa) and a histidine-containing phosphocarrier protein (HPr) as model proteins [35], we now discuss the consequences of unfolded βLGa and HPr translocation in silicon nitride nanopores. In addition, we discuss and compare the difference between folded and unfolded protein translocation kinetics.

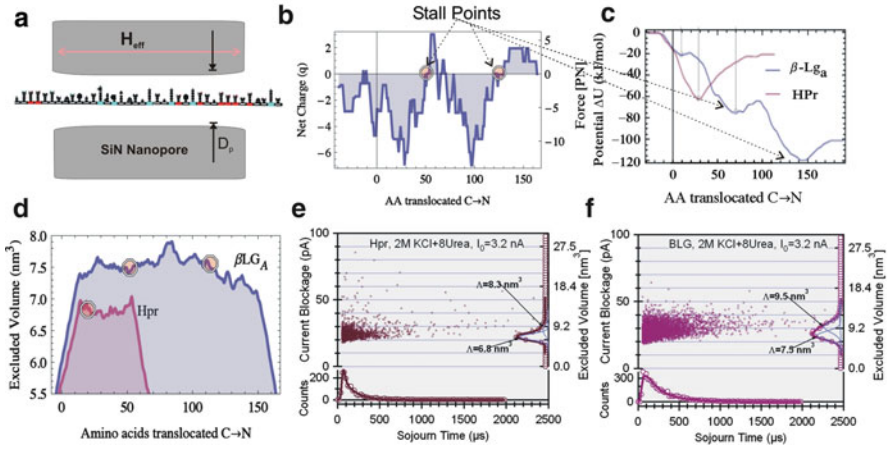

Fig. 6.5 (**a**) Schematic of linear translocation for βGLa. (**b**) The net charge of βGLa as predicted by treating the ionization of the individual residues as independent at pH 7.0 as a function of AA number. (**c**) The electrostatic contribution to the potential energy of βGLa and Hpr as a function of AA through the nanopore. This potential is for the C terminus entering first. (**d**) The calculated excluded partial volume Λ profile for ββGLa and Hpr proteins as a function of number of amino acids (AA) translocated. The slopes on the *left* and *right sides* show the insertion and exit of the linear chain. The *circles* mark the location of stall points (charge zero) during the translocation. Event Scatter Plot and marginal distributions of Sojourn Times and Calibrated Excluded Volume for βGLa and (**e**) HPr (**f**) in a small-diameter nanopore (D_p~4 nm) under denaturing conditions (8 M urea). The open pore current was the same (I_o=3.2 nA) during these measurements. βGLa (PDB file 2AKQ, 73,549.60 kDa) has 162 amino acids and it has a charge of ~8*e* at pH 7. HPr (PDB file 1POH, 9121.54 Da) has 85 aa and it has a charge of −2e at pH 7. The pore effective thickness H_{eff}=20 nm was used for all calculations

6.5.1 Stall Point Potential Well Model

Due to the heterogeneous distribution of charged amino acids, the calculated net charge of a segment of a βLGa polypeptide chain, $Q_{AA} = \sum q_i$ *in the pore*, can be positive, negative and zero as a function of the number of residues translocating in a pore as shown in Fig. 6.5b. Locations where the net charge or force is zero, we call stall points. The positive and negative net charge positions in the curve imply that at these positions during the linear translocation the electrophoretic force, $Fe = Q_{AA}\Psi/H_{eff}$, can either oppose or drive the translocation. This can be seen more clearly in the translocation potential plot in Fig. 6.5c. The potential profile is calculated by

$$\Delta U(x) = \int_0^x \frac{\Psi}{H_{eff}} q(x)dx. \tag{6.5}$$

The potential profile plot shows that βLGa has two stall points and Hpr has one. Near the stall points, the peptide chain is likely thermally fluctuating in the potential well that is formed due to the polypeptide charge sequence. If the potential well is deep enough, the unfolded protein will be metastably trapped in the nanopore; the translocation process would still go forward eventually because the total electrical driving force is downhill. While the unfolded protein is trapped at a stall point, its escape is thermally activated. The total translocation will therefore be a combination of electrophoretic and thermally activated processes.

6.5.2 The Excluded Volume at Stall Points

Due to the large atomic volume variations between amino acids (up to 3.8 times) the instantaneous excluded volume profile of an unfolded protein translocation, $\Lambda_{AA} = \sum V_{Ai}$, is a function of the protein primary sequence as shown in Fig. 6.5d. βLGa has more large volume amino acids, V_{Ai}, compared to HPr, thus the calculated excluded volume (Λ_{AA}) for βLGa is larger compared to HPr. The measured excluded volume is a time average of the local segment volume. Since the polypeptide chain dwells in the pore longer at the stall points, the corresponding excluded volume at the stall points (red circles in Fig. 6.5d) should have more weight. Since the purely electrophoretic part of the translocation should contribute ~1–2 μs to the translocation time of these small single-domain proteins, the net translocation time is likely dominated by the sojourns at the stall points. Thus the experimentally determined excluded volume should correspond to the stall point volumes.

The experimental data measured in the same ~4 nm diameter pore for βLGa (Fig. 6.5e) and HPr (Fig. 6.5f) under denatured conditions (8 M urea) show that the peak value of the mean ΔI_b is indeed larger for βLGa than HPr supporting this analysis. The volumes measured from the peak values of ΔI_b data match

quantitatively with the volume calculated at the stall points for the βGLa and HPr in Fig. 6.5d (right axis). The broader distribution of ΔI_b for βLGa is likely caused by contributions from the translocation of looped configurations due to the presence of disulfide bonds in βLGa [35].

6.5.3 *Parameters Affecting the Linear Translocation Potential*

The net charge profile Q_{AA} is not only a function of protein primary charge sequence, it also depends on the nanopore effective length H_{eff} and solution pH as illustrated in Fig. 6.6. Changing the thickness of the pore changes the length of the segment of the unfolded protein that is exposed to the nanopore environment. The translocation potential changes significantly with pore thickness because of the changes in coarse grain sampling of the local structure. In this case, changing the pore thickness will change the presence or absence of stall points. In the limit of thick pores, $l_m < H_{eff}$, there will be no stall points.

Varying solution pH systematically changes the charge sequence of the same protein to vary the electrostatic translocation potential. Changing the pH alters the number, depth, and location of stall points along the polypeptide chain as shown in Fig. 6.6b for bacterial L-lactate dehydrogenase.

In addition, the depth of the potential well $\Delta U^{\ddagger}$ is deeper or the barrier height is larger at a higher voltage. This analysis implies the linear translocation potential profile depends on the protein charge sequence, nanopore thickness, solution pH, and applied voltage.

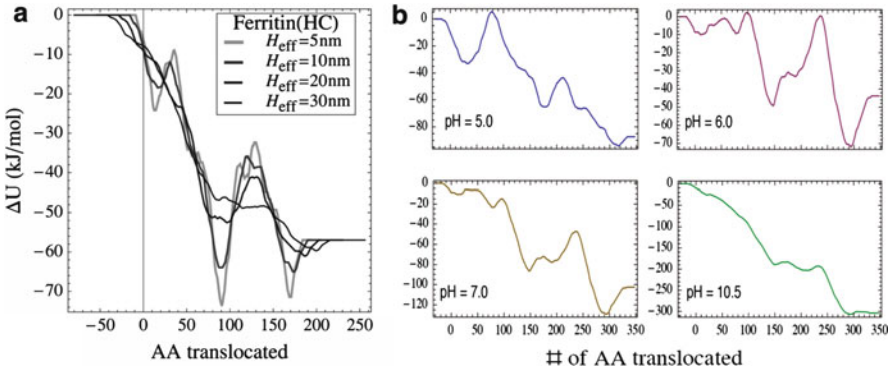

Fig. 6.6 Nanopore length H_{eff} and solution pH effects on translocation potential profile: (**a**) translocation potential profile at four different pore thicknesses (H_{eff}=5, 10, 20, 30 nm) for ferritin heavy chain (PDB file: *2Z6M, 176 aa*). (**b**) The predicted potentials for linear translocation of bacterial L-lactate dehydrogenase (PDB file: *1LLD, 319 aa*) through a 10 nm pore at pH=5.0, 6.0, 7.0, and 10.5 as labeled in the figure

6.6 Comparison of Time Histograms

For a linear amino acid chain translocation as shown in Fig. 6.5a, if there are neutral regions or stall points, Eq. (6.3) is no longer valid. If the potential wells are deep enough, Kramers reaction rate theory [40] predicts that the distribution of sojourn times should be multi-exponential according to the number of barriers present. When there is only one barrier present, using a simple one dimensional transition state theory, the predicted escape time from one electrostatic trap with barrier height ($\Delta U^{\ddagger}$) will be

$$t^{-1} \propto \exp(-\Delta U^{\ddagger}/k_B T) \tag{6.6}$$

This neglects protein conformational changes that could provide alternate lower-barrier pathways.

As shown in Fig. 6.5c, there is one stall point for Hpr and two for βLGa. The time histograms measured for these two proteins under denaturing conditions show that the t_d histogram of Hpr (Fig. 6.7a) fits well with a single exponential, and the t_d histogram of βLGa (Fig. 6.7b) fits better with two exponentials. This is consistent with the presence of no more than two stall points during translocation of these two proteins.

It is enlightening to compare the time histograms of heterogeneously charged polypeptides with homogeneously charged dsDNA. Without any stall points, due to their uniform charge density, the time histograms shown for a 2.7 kb (Fig. 6.7c) and a 7 kb (Fig. 6.7d) DNA fit well to the analytical model predicted in Eq. (6.4).

The DNA molecules translocate through a nanopore moving on average at the molecule's terminal velocity with variance increasing linearly with t_d according to $<x^2>=2Dt_d=2(k_bT/)t_d$. In this case, the most probable time will be the length divided by its average velocity, $t_d=l_m/v$ ($l_m>>H_{eff}$). Thus a longer t_d is expected and observed for the 7 kb DNA (Fig. 6.8d) compare to the 2.7 kb.

The time distribution described in Eq. (6.4) derived for a charged particle is appropriate to fit the time distribution of BSA. In this case, l_m~14 nm<H_{eff}=20 nm, $d=H_{eff}$=20 nm. Indeed the Eq. (6.4) fits well for the time histograms of BSA at pH 7 (Fig. 6.7e) and pH 4.5 (Fig. 6.7f). These time histograms of the native state BSA at pH 7 (Fig. 6.7e) and at pH 4.5 (Fig. 6.7f) are from the cluster one events in Fig. 6.4d, e, respectively. These fits suggest that native state BSA translocation can be treated under the simple charged particle model.

The above analyses have made many simplifying assumptions and neglected many complex issues including neglect of: conformational changes during the translocation process, protein interactions with the nanopore wall, dynamics of long, floppy segments of the molecule outside of the pore, the surface charge of a nanopore and electroosmosis. Nevertheless, the simple models have thus far been able to quantitatively explain the protein translocation data.

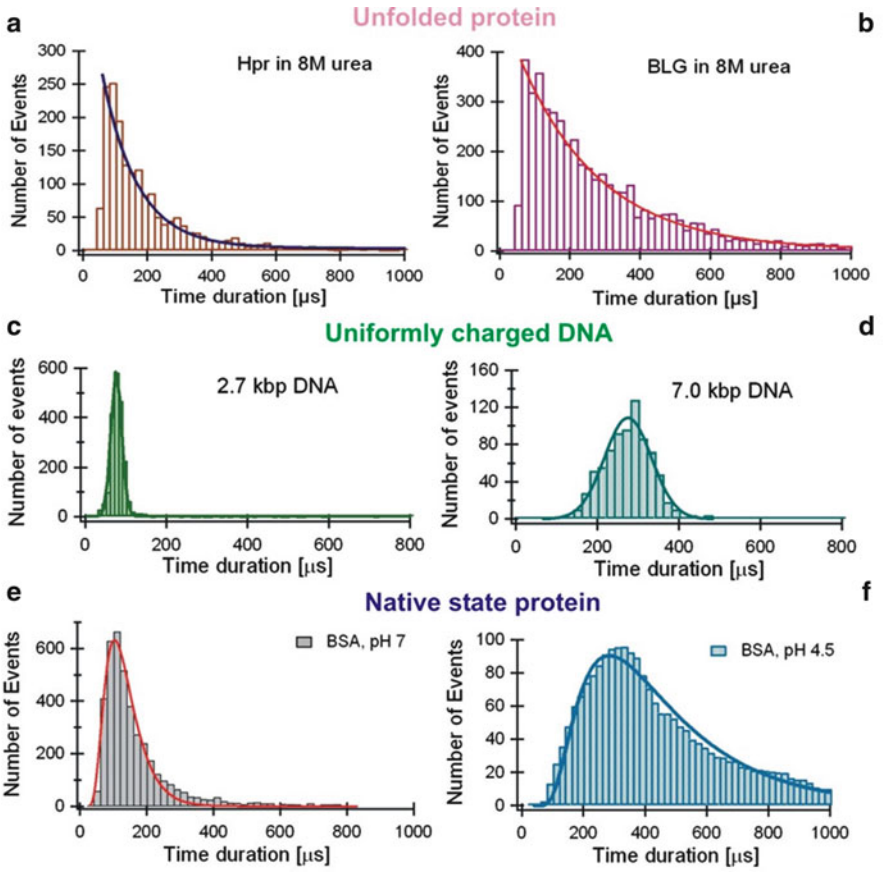

Fig. 6.7 *Time duration histograms of* unfolded proteins with Hpr that has one stalling point (**a**) and βGLa that has two stalling points (**b**); uniformly charged dsDNA with no stall point: 2.7 kb (**c**) and 7.0 kb (**d**); native state BSA as a charged particle at pH 7 (**e**) and pH 4.5 (**f**). The *solid curves* are fittings to exponentials for unfolded proteins (**a**) and (**b**). The rest of the panels are fittings to Eq. (6.6) and the pore effective thickness H_{eff}=20 nm was used for the fittings

6.7 Summary

Nanopore translocation of native state protein molecules can be treated as the biased 1D diffusion of simple charged particles if the proteins are stable with respect to electrostatically induced denaturation. Uniformly charged polymer translocation also follows 1D biased diffusion. The kinetic behavior of unfolded protein translocation is highly dependent on the sequence of charged residues. These observations are in sharp contrast to DNA translocation. When calculating the driving force for DNA translocation, the thickness of the pore cancels out because of the uniform charge density; there is essentially no DNA sequence effect on the translocation

driving force. The distribution of translocation times depends strongly on protein sequence, applied voltage ψ, as well as H_{eff}.

In summary, our studies of single protein translocation in solid-state nanopores have shown that:

1. A nanopore experiment can measure a protein's size, electrical charge, and conformation state.
2. If a native state protein has enough disulfide bonds (e.g. BSA has 17) to keep the protein intact inside a nanopore in spite of the high electric field strength, the protein translocates through the nanopore like a simple charged particle.
3. If a protein is completely unfolded as an amino acid chain, the translocation kinetics is highly sequence dependent.
4. It is possible to distinguish proteins based on their nanopore translocation signal profile in their native and unfolded state as functions of pH (charge state) and applied voltage (driving force).
5. Furthermore, based on our analysis, an advantage of the nanopore experiment is that it has the potential to distinguish proteins with single or multi-site mutants. We describe this possibility in details below.

6.8 Future Trends

The sensitivity of the ionic current signal $\Delta I_b(t)$ to the charge and volume of specific segments of the polypeptide chain present inside the nanopore at the stall points suggests that unfolded protein translocation could ultimately provide enough contrast to routinely distinguish different proteins in complicated mixtures. The compatibility of nanopores with microfluidics and their ability to obtain data from zeptomole samples suggest that these approaches could be used to screen single cell or subcellular samples. To illustrate these ideas we report some proof-of-concept calculations.

6.8.1 Nanopore Protein Mixture Screening

Using staphylococcal nuclease (SNase) as a model protein, we predict the nanopore translocation profiles of several SNase mutants and envision the results from a set of nanopore measurement as illustrated in Fig. 6.8.

Staphylococcal nuclease (SNase, Fig. 6.8a) Consists of a polypeptide chain of 149 amino acid residues without disulfide binds [41, 42]. SNase has been used as a model protein to study protein folding and unfolding. More than 500 mutants have been made and characterized in order to study the sequence dependence of its structure and function.

Varying Protein charge Sequence allows control of the magnitude of specific barriers in the translocation profile and can provide insight into the translocation time distribution. Fig. 6.8b illustrates how protein charge sequence changes alter

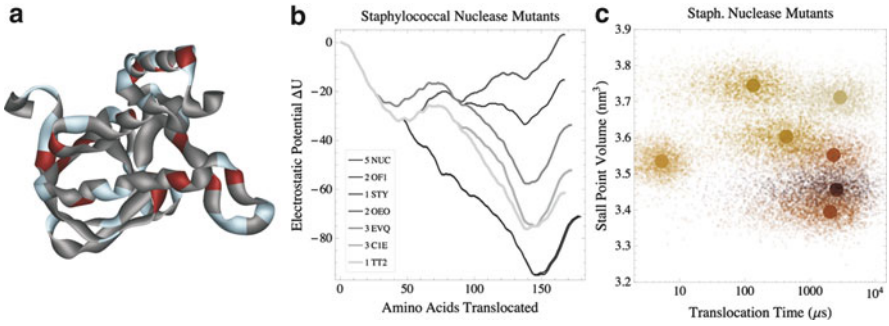

Fig. 6.8 (**a**) Structure of wild type SNase with basic (positive at pH 7.8) residues labeled *dark* and acidic (negative at pH 7.8) residues labeled *light grey*. (**b**) Electrostatic contribution to translocation potential for several mutants of SNase at pH 7.8 illustrating how sequence can change the location, number, and depth of electrostatic barriers. (**c**) Future nanopore measurement with improved signal to noise ratio would allow of distinguishing single site mutant proteins

the barriers present during translocation. The linear translocation of seven selected SNase mutants in a nanopore at pH. 7.8 (Fig. 6.8b) shows their electrical potential profiles vary significantly. The potential well depth or barrier height could vary by a factor of 5 between the SNase mutants.

Varying the electrostatic potential allows changing the electrical potential barrier height $\Delta U^{\ddagger}$ values systematically. Systematically changing the electrical potential barrier height $\Delta U^{\ddagger}$ values will change the protein dwell time t_d in a pore as described in Eq. (6.5). Our data analysis tools have enabled us to predict a 2D map of stall point volumes (Λ_{AA}) vs. time durations (t_d) shown in Fig. 6.8c from a future nanopore measurement of these SNase mutant proteins.

A 2D map illustrated in Fig. 6.8c, in principle, would be able to detect single site or multi-site mutants. Furthermore, a 2D map of excluded volume (Λ or ΔI_b) and time duration (t_d) measured under different pH and voltage could allow identification and resolution of proteins.

6.8.2 *Open Challenges*

Several challenges must be overcome to make the 2D map in Fig. 6.8c become a reality. One of such challenges is to find the correlation between protein primary charge sequence and the dwell time or the theoretical connection between the measured distributions of translocation times with the sequence and structural properties of the proteins.

At the present time, a quantitative theory for phenomenon of protein dwell time in a nanopore is not available and systematic studies of the sequence and condition effects on protein translocation are almost non-existent. As a result, a full explanation of the dwell time distribution remains an unsolved problem.

The current blockage signal from a nanopore measurement contains the information on the protein's shape or folding state and on the sequence of the amino-acid volume and charge of the local segment of the polypeptide chain in the pore if the protein molecule is unfolded. The research on using solid-state nanopores to measure the shape of single protein molecules at different folding states and to probe its charge sequence when it is unfolded in salt solution is still at a very early stage.

Equations (6.1), (6.3) and (6.4) were developed using several assumptions including: (1) a uniform distribution of charge on the protein, (2). the protein is a small hard sphere, (3) the protein does not interact with the pore walls, and (4) there is only one ionization state of the protein. These assumptions limit the general applicability of these equations. Future work must evaluate the need for corrections for these assumptions to enable a better description of protein translocation.

Complicated assemblies of proteins such as laminin produce complex signals that cannot be uniquely interpreted. For example, the recorded current trace (Fig. 6.1c) for Laminin protein shows the complexity of the signal measured for a partially denatured protein. At the present time, we are still developing analysis routines to process these more complicated data sets. In this chapter we only attempted to discuss the current blockage signal produced by proteins in two simplest conformations: in their native state and in their completely unfolded state.

Future developments of nanopore techniques for sensing proteins should be focused on improvement of signal-to-noise, understanding of protein translocation signal and protein structure, dynamic adjustment of DC bias potential, control of nanopore surface chemistry, in situ characterization of nanopore geometry and electrical response, analysis improvements to provide richer translocation data, and incorporation of other single molecule methods into the nanopore experiments.

Acknowledgments We thank Professor J. Golovchenko and Harvard nanopore group for nanopore fabrication, Ryan Rollings, Edward W. Graef Jr., Denis F. Tita, and Errol Porter for nanopore fabrication and characterization. We acknowledge the funding support provided by NHGRI/NIH R21HG003290, NHGRI/NIH R21HG00477, NSF/MRSEC 080054, ABI-111/710, and NIH R01GM071684 to DST.

References

1. Rapoport, T.A., *Protein translocation across the eukaryotic endoplasmic reticulum and bacterial plasma membranes*. Nature, 2007. 450(29): p. 663–669.
2. Wickner, W. and R. Schekman, *Protein Translocation Across Biological Membranes*. Science, 2005. 310(5753): p. 1452–1456.
3. Simon, S.M. and G. Blobel, *A protein-conducting channel in the endoplasmic reticulum*. 1991. 65(3): p. 371–380.
4. Sutherland, T.C., Y.-T. Long, R.-l. Stefureac, I. Bediako-Amoa, H.-B. Kraatz and J.S. Lee, *Structure of Peptides Investigated by Nanopore Analysis*. Nano Lett, 2004. 4(7): p. 1273–1277.

5. Stefureac, R., L. Waldner, P. Howard and J.S. Lee, *Nanopore Analysis of a Small 86-Residue Protein*. Small, 2008. 4(1): p. 59–63
6. Oukhaled, G., J. Mathe, A.L. Biance, L. Bacri, J.M. Betton, D. Lairez, J. Pelta and L. Auvray, *Unfolding of Proteins and Long Transient Conformations Detected by Single Nanopore Recording*. Physical Review Letters, 2007. 98(15): p. 158101–4
7. Pastoriza-Gallego, G.G. M., B. Thiebot, J.-M. Betton and J. Pelta, *Polyelectrolyte and unfolded protein pore entrance depends on the pore geometry*. Biochimica et Biophysica Acta - Biomembranes 2009. 1788: p. 1377–1386.
8. Mohammad, S. Prakash, A. Matouschek and L. Movileanu, *Controlling a Single Protein in a Nanopore through Electrostatic Traps*. Journal of the American Chemical Society, 2008. 130(12): p. 4081–4088.
9. Movileanu, L., S. Howorka, O. Braha and H. Bayley, *Detecting protein analytes that modulate transmembrane movement of a polymer chain within a single protein pore*. Nat Biotech, 2000. 18(10): p. 1091–1095.
10. Han, A., G. Schurman, G. Mondin, R.A. Bitterli, N.G. Hegelbach, N.F. de Rooij and U. Staufer, *Sensing protein molecules using nanofabricated pores*. APPLIED PHYSICS LETTER, 2006. 88: p. 093901–3.
11. Han, A., M. Creus, G. Schurmann, V. Linder, T.R. Ward, N.F. de Rooij and U. Staufer, *Label-Free Detection of Single Protein Molecules and Protein−Protein Interactions Using Synthetic Nanopores*. Analytical Chemistry, 2008. 80(12): p. 4651–4658%U ac7025207http://dx.doi.org/10.1021/ac7025207.
12. Fologea, D., B. Ledden, D.S. McNabb and J. Li, *Electrical Characterization of Protein Molecules by a Solid-State Nanopore*. APPLIED PHYSICS LETTERS, 2007. 91.
13. Talaga, D.S. and J. Li, *Single-Molecule Protein Unfolding in Solid State Nanopores*. Journal of American Chemical Society, 2009. 131(26): p. 9287–9297.
14. Firnkes, M., D. Pedone, J. Knezevic, M. Döblinger and U. Rant, *Electrically Facilitated Translocations of Proteins through Silicon Nitride Nanopores: Conjoint and Competitive Action of Diffusion, Electrophoresis, and Electroosmosis*. Nano Letters, 2010. 10(6): p. 2162–2167.
15. Niedzwiecki, D.J., J. Grazul and L. Movileanu, *Single-Molecule Observation of Protein Adsorption onto an Inorganic Surface*. Journal of the American Chemical Society, 2010. 132(31): p. 10816–10822.
16. Li, J., M. Gershow, D. Stein, E. Brandin and J.A. Golovchenko, *DNA Molecules and Configurations in a Solid-state Nanopore Microscope*. Nat. Mater., 2003. 2: p. 611–615.
17. Bezrukov, S.M., *Ion Channels as Molecular Coulter Counters to Probe Metabolite Transport*. Journal of Membrane Biology, 2000. 174(1): p. 1–13.
18. DeBlois, R.W. and C.P. Bean, *Counting and Sizing of Submicron Particles by the Resistive Pulse Technique*. Review of Scientific Instruments, 1970. 41(7): p. 909.
19. Gregg, E.C. and k.D. Steidley, *Electrical Counting and Sizing of Mammalian Cells in Suspension*. Biophysical Journal, 1965. 5(4): p. 393–405.
20. Henriquez, R.R., T. Ito, L. Sun and R.M. Crooks, *The resurgence of Coulter counting for analyzing nanoscale objects*. The Analyst, 2004. 2004(129): p. 478–482.
21. Smeets, R.M., U.F. Keyser, D. Krapf, M.-Y. Wu, D. Nynke H and C. Dekker, *Salt Dependence of Ion Transport and DNA Translocation through Solid-state nanopores*. Nano Lett., 2006. 6 (1): p. 89–95.
22. King, G.M. and J.A. Golovchenko, *Probing Nanotube-Nanopore Interactions*. Physical Review Letters, 2005. 95(21): p. 216103.
23. Levadny, V., V.M. Aguilella and M. Belaya, *Access resistance of a single conducting membrane channel*. Biochimica et Biophysica Acta (BBA) - Biomembranes, 1998. 1368(2): p. 338–342.
24. Vodyanoy, I. and S.M. Bezrukov, *Sizing of an ion pore by access resistance measurements*. Biophysical Journal, 1992. 62(1): p. 10–11.
25. Dekker, C., *Solid-state nanopores*. Nature Nanotechnology, 2007. 2: p. 209–215.

26. Healy, K., B. Schiedt and A.P. Morrison, *Solid-state nanopore technologies for nanopore-based DNA analysis*. Nanomedicine, 2007. 2(6): p. 875–897.
27. Li, J., D. Stein, C. McMullan, D. Branton, M.J. Aziz and J.A. Golovchenko, *Ion-beam sculpting at nanometre length scales*. Nature, 2001. 412(12 July): p. 166–169.
28. Gierhart, B.C., D.G. Howitt, S.J. Chen, Z. Zhu, D.E. Kotecki, R.L. Smith and S.D. Collins, *Nanopore with Transverse Nanoelectrodes for Electrical Characterization and Sequencing of DNA*, in *The 14th International Conference on Solid-State Sensors, Actuators and Microsystems*. 2007, Transducers & Eurosensors: Lyon, France.
29. Stein, D., J. Li and J.A. Golovchenko, *Ion-Beam Sculpting Time Scales*. Physical Review Letters, 2002. 89(27).
30. Storm, A.J., J.H. Chen, X.S. Ling, H.W. Zandbergen and C. Dekker, *Fabrication of solid-state nanopores with single-nanometre precision*. Nature Materials, 2003. 2: p. 537–540.
31. Venkatesan, B.M., B. Dorvel, S. Yemenicioglu, N. Watkins, I. Petrov and R. Bashir, *Highly Sensitive, Mechanically Stable Nanopore Sensors for DNA Analysis*. Adv. Mater., 2009. 21: p. 1–6.
32. Venkatesan, B.M., A.B. Shah, J.-M. Zuo and R. Bashir, *DNA Sensing Using Nanocrystalline Surface-Enhanced Al_2O_3 Nanopore Sensors*. Adv. Funct. Mater., 2010. 20: p. 1266–1275.
33. Stein, D.M., C.J. McMullan, J. Li and J.A. Golovchenko, *Feedback-controlled ion beam sculpting apparatus*. Review of Scientific Instruments, 2004. 75(4): p. 900–905.
34. Cai, Ledden, Krueger, Golovchenko and Li, *Nanopore sculpting with noble gas ions*. Journal of Applied Physics, 2006. 100.
35. Talaga, D. and J. Li, *Single-molecule protein unfolding in solid state nanopores*. J. Am. Chem. Soc., 2009. 131: p. 9287–9297.
36. Fologea, D., B. Ledden, D.S. McNabb and J. Li, *Electrical Characterization of Protein Molecules in a Solid-State Nanopore*. Appl. Phys. Lett., 2007. 91.
37. Peters, T., Jr., *Serum Albumin*. Adv. Protein Chem., 1985. 37: p. 161–245.
38. Collins, B.E., K.-P.S. Dancil, G. Abbi and M.J. Sailor, *Determining Protein Size Using an Electrochemically Machined Pore Gradient in Silicon*. Advanced Functional Material, 2002. 12 (3): p. 187–191.
39. Bloomfield, V., *The Structure of Bovine Serum Albumin at Low pH*. Biochemistry, 1966. 5(2): p. 684–689.
40. Kramers, H.A., *Brownian motion in a field of force and the diffusion model of chemical reactions*. Physica (Utrecht), 1940. 7: p. 284–304.
41. Cotton, F.A., J. Edward E. Hazen and M.J. Legg, *Staphylococcal nuclease: Proposed mechanism of action based on structure of enzyme—thymidine 3′,5′-bisphosphate—calcium ion complex at 1.5-A° resolution* Proc. Nati. Acad. Sci. USA, 1979. 76(6): p. 2551–2555.
42. Tucker, P.W., E.E. Hazen and F.A. Cotton, *Staphylococcal nuclease reviewed: A prototypic study in contemporary enzymology* Molecular and Cellular Biochemistry, 1979. 23(3).